Observation of the Fast Potential Change at L-H Transition by a Heavy-Ion-Beam Probe on JFT-2M

T. Ido,[1] K. Kamiya,[2] Y. Miura,[2] Y. Hamada,[1] A. Nishizawa,[1] and Y. Kawasumi[1]
[1]*National Institute for Fusion Science, Oroshi, Toki, 509-5292, Japan*
[2]*Japan Atomic Energy Research Institute, Tokai, Naka, Ibaraki, 319-1195, Japan*
(Received 17 September 1999; published 22 January 2002)

The fast potential change near the separatrix is measured directly at the L-H transition by a heavy-ion-beam probe. The potential changes with two different time scales at the L-H transition triggered by a sawtooth crash: it drops at first with the time scale of 10−100 μs just after the arrival of the heat pulse due to the sawtooth crash. Then, it decreases again at a few 100 μs after the first drop at a time scale of about 200 μs.

DOI: 10.1103/PhysRevLett.88.055006 PACS numbers: 52.55.Fa

The important role of radial electric field (E_r) in the confinement of tokamak plasmas was pointed out [1] in a process to clarify the physical mechanism of H mode discovered first in ASDEX [2]. After the following theoretical [3] and experimental [4,5] studies, it has been claimed in numerous works that E_r is closely connected to L-H transition [6]. Lately the suppression of the turbulence by sheared $\mathbf{E} \times \mathbf{B}$ flow [7] is the most credible model for the improved confinement. For the purpose of clarifying the causality between the formation of E_r and the improved confinement, the temporal behaviors of E_r are observed [8–12]. The measurement of the time scale of E_r change itself as well as the causality is important in order to identify the physical mechanism of the formation of E_r because the time scale is determined by the radial current which forms E_r. However, the previous studies are not necessarily enough to study the temporal behavior of E_r because E_r is not measured directly and the time resolutions, $\geq$50 μs, are possibly not enough, judging from the theoretical predictions [3,13]. Therefore, a heavy-ion-beam probe (HIBP) [14] has been installed to observe the temporal behavior of E_r with a high time resolution in JFT-2M tokamak.

HIBP can measure a local electrostatic potential (ϕ) directly even in high temperature plasmas with a high time resolution. Singly charged heavy ion beam, called the primary beam, is injected into the magnetically confined plasma (Fig. 1). A part of the primary beam is charged doubly through the electron impact ionization and it is called the secondary beam. Since the charge number increases by one, the total energy of the injected ion changes by the potential energy at the ionization point. Therefore, ϕ at the ionization point can be obtained through the measurement of the difference of the kinetic energies between the primary and the secondary beam ion [Fig. 1(a)]. The secondary beam current (I_s) is large enough to measure ϕ with a high time resolution of about 1 μs. Moreover, the fluctuation of I_s ($\tilde{I}_s$) reflects the density fluctuation ($\tilde{n}_e$), although the fluctuation of the electron density (n_e) and temperature (T_e) on the beam trajectory must be taken into account. Therefore, an HIBP is useful to study the physical mechanism of improved confinements which may relate the suppression of $\tilde{n}_e$ by sheared $\mathbf{E} \times \mathbf{B}$ flow [15].

We have installed a 500 keV HIBP [16], which was previously used in JIPP T-IIU tokamak [17], on JFT-2M. It can measure ϕ with the time resolution of about 2 μs. We observed that the change in ϕ at an L-H transition triggered by a sawtooth crash could be as fast as 10 μs [18]. This Letter presents the observation of temporal behaviors of ϕ at L-H transitions triggered by a sawtooth heat pulse and discusses the time scales for the first time.

JFT-2M is a medium-sized tokamak with a major radius (R) of 1.3 m and an averaged minor radius (a) of 0.3 m. The experiments are performed with the toroidal magnetic field of 1.2 T, the plasma current of 190 kA, an upper single null divertor configuration, the ion ∇B drift is toward the X point, and the line averaged electron density of 3.5×10^{19} m^{-3} just before the L-H transition. The neutral beam (NB) is injected in the codirection.

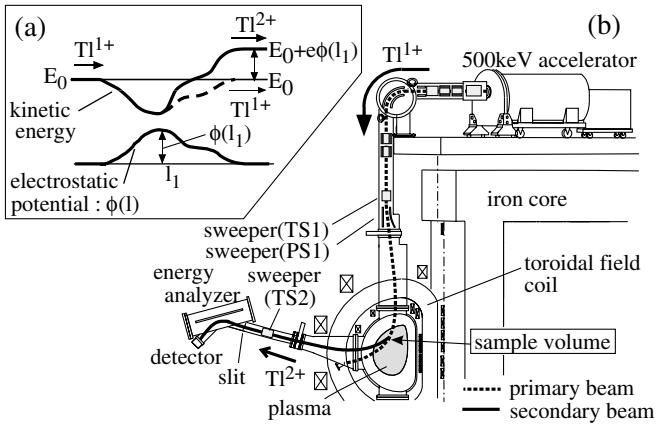

FIG. 1. (a) The principle of potential measurement. The horizontal axis is the distance along the beam trajectory and l_1 indicates the position of ionization of the primary beam. The secondary beam ion (Tl^{2+}) gains $e\phi(l_1)$ due to the ionization. (b) Schematic view of JFT-2M HIBP.

The thallium ions with the energy of 350 keV are injected for the HIBP measurement. The kinetic energy of the secondary beam is measured by using a electrostatic parallel plate analyzer [19]. Therefore, the change in the out-of-plane entrance angle to the analyzer, which corresponds to the deflection of the beam in the toroidal angle caused by the change in the poloidal magnetic field, causes a severe error in the measurement of the energy. In JFT-2M HIBP, two toroidal sweepers [TS1 and TS2 shown in Fig. 1(a)] are installed in order to tune the out-of-plane entrance angle, and the error is suppressed to 16 V or less at the L-H transition.

The position of the sample volume of the HIBP can be selected by the radial sweep of the primary beam. The radial width of the sample volume is about 6 mm according to a trajectory calculation with the phase space volume of the injected beam [20]. As mentioned above, $\tilde{n}_e$ is observed through $\tilde{I}_s$. Since the sampling rate is 5 μs, the Nyquist frequency is 100 kHz. In the observation near the separatrix, however, I_s also depends on T_e because the ionization rate also depends on T_e when $T_e < 100$ eV [21]. Moreover, it should be noted that I_s depends on the attenuation of the beam on the trajectory.

Figure 2 shows the temporal history of soft x ray (SX) and deuterium Balmer α line (D_α) intensities at an L-H transition and profiles of ϕ. The NB injection (NBI) is switched on at 700 ms and its power is 840 kW, which is much larger than the L-H threshold power. The period of sawteeth oscillation is about 15 ms. The SX intensity from the scrape off layer (SOL) and D_α intensity drop rapidly after a sawtooth crash at 750.4 ms. The L-H transition is triggered clearly by a sawtooth crash. Figure 2(d) shows the profiles of ϕ measured through the radial sweep of the sample volume from the core to the edge with a sweep rate of 0.66 mm/μs and with a repetition frequency of 2 kHz. The hatched periods in Figs. 2(a)–2(c) correspond to the measurement of the profiles. The position of the sample volume is expressed in terms of the distance from the separatrix on the midplane (ds). Actually, the sample volumes are not on the midplane and the positions are mapped on the midplane by assuming that ϕ is equal on a magnetic surface. The profiles of I_s are also shown in Fig. 2(d). The steep gradient in the profile reflects the steep gradient of the electron pressure, and it may indicate the possible position of the separatrix. The decrease in ϕ at the L-H transition is about 300 V at the edge, which is in agreement with the previous results measured by toroidal and poloidal rotations and pressure gradient [22]. The gradient of ϕ changes in the narrow region of about 1.5 cm near the separatrix and it becomes $27 \pm 4kV/m$.

The fast temporal behaviors of ϕ can be measured at fixed positions with the radial sweep voltage fixed. The change in ϕ near the separatrix is shown in Fig. 3. The experimental condition is the same as that of Fig. 2. When the heat pulse reaches to the plasma edge, the ϕ jumps in the positive direction at first. The D_α intensity increases simultaneously, and the magnetic fluctuation is also enhanced. Since we observed the increase in electron saturation current on the divertor plate at that time, the positive

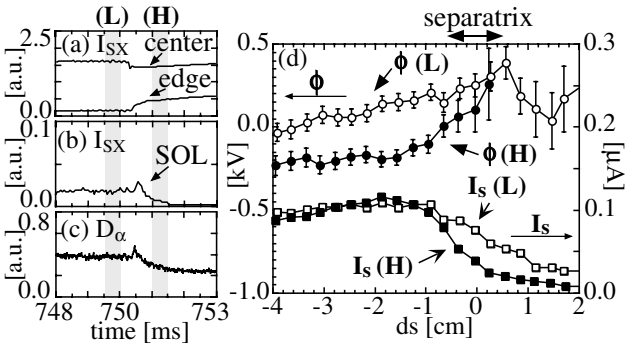

FIG. 2. (a) Chord integrated soft x-ray (SX) intensities from the core ($q \sim 1$) and the edge ($\rho \sim 0.85$) where ρ is the distance of the chord from the plasma center normalized by the minor radius. (b) SX intensity from SOL ($\rho \sim 1.1$). The hatched periods indicate the measurement time of the potential profile shown in (d). (c) D_α intensity in the divertor. (d) Potential (ϕ) and the secondary beam intensity (I_s) profiles of L and H mode. The negative sign in the horizontal axis means the inside of the separatrix.

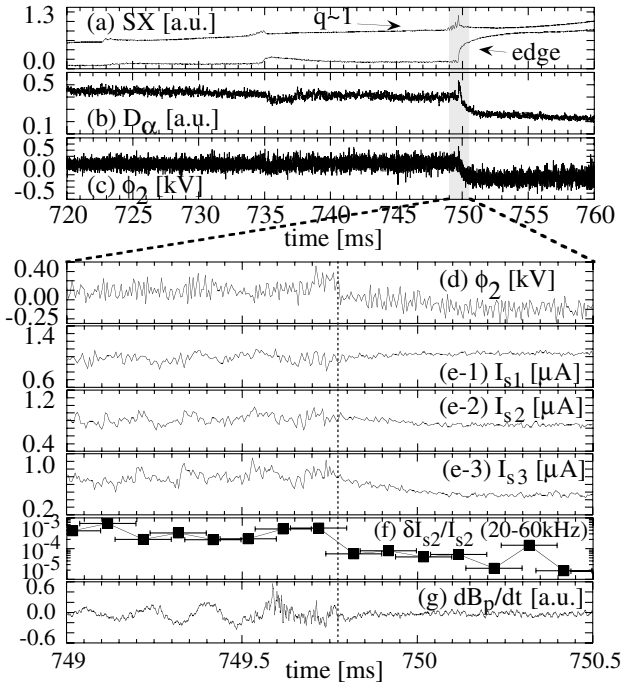

FIG. 3. The fastest temporal evolution of potential and other plasma parameters at L-H transition. The positions of sample volumes are $ds = -2.0$, -1.3, and -1.0 cm for ch. 1, 2, and 3. (a) SX intensities from the core and the edge. (b) D_α intensity. (c), (d) the potential of ch. 2. (e-1), (e-2), and (e-3) show the secondary beam intensities of ch. 1, 2, and 3, respectively. (f) The power of fluctuation of the secondary beam of ch. 2 integrated from 20 to 60 kHz in frequency. (g) the magnetic probe signal. The dotted line indicates the time when the potential drops rapidly.

jump might be caused by the electron loss due to the magnetic fluctuation induced by the sawtooth crash. After that, the drop of about 150 V in ϕ occurs very rapidly within 10 μs. $\tilde{I}_s$ in the frequency range of 100 kHz or less and the magnetic fluctuation are also suppressed at the same time. I_s of ch. 1 [Fig. 3(e-1)] starts increasing, though that of ch. 3 [Fig. 3(e-3)] starts decreasing. They indicate the increase in n_e and/or T_e at $ds = -2.0$ cm, and/or the decrease in the attenuation of the beam through the decrease in n_e and/or T_e in the outer region. Anyhow, they show the formation of the steep gradient of n_e and/or T_e which indicates the formation of the transport barrier. The ϕ also changes further to about -200 V, which is the steady level in ELM-free H modes, during the formation of the transport barrier.

Figure 4 shows ϕ changes by two steps (746.7–747 and 747.8–748.6 ms) with a short stagnation (747–747.8 ms) clearly, though the experimental condition is the same as that of Fig. 3. The observation position is different from that of Fig. 3, however the similar behavior to that in Fig. 3 without stagnation also occurs at the position in the other shot. Therefore, whether the two steps appear or not is not due to the observation position, and Figs. 3 and 4 are shown here because they are a series of shots with the same experimental condition. Just after the sawtooth crash at 746.7 ms, ϕ and $\tilde{I}_s$ with the frequency range of 60 kHz or less is suppressed [Fig. 4(e)]. After that, however, the fluctuation level in the frequency range from 80 to 100 kHz increases as shown in Fig. 4(f) and ϕ stagnates for about 1 ms. During the stagnation, the increase in the edge SX intensity shows n_e and T_e continue to increase [Fig. 4(a)]. After that, although no event such as a sawtooth crash occurs, the ϕ starts decreasing with the relatively slow time scale at 747.8 ms and the SOL SX and D_α intensities further decrease at that time [Figs. 4(b) and 4(c)]. They show the confinement is also improved further at that time. This sort of change at about 1 ms after a sawtooth crash is also observed in the case of L-H transition triggered by a small heat pulse as shown in Ref. [23]. The change in ϕ is closely related to the decrease of $\tilde{n}_e$ in Figs. 3 and 4. However, we cannot conclude yet on the causality among the change in E_r, the suppression of turbulence, and the improved confinement, because there is no clear time lag among them and the frequency range of the measurement may be insufficient compared with the Doppler shift due to the $\mathbf{E} \times \mathbf{B}$ flow.

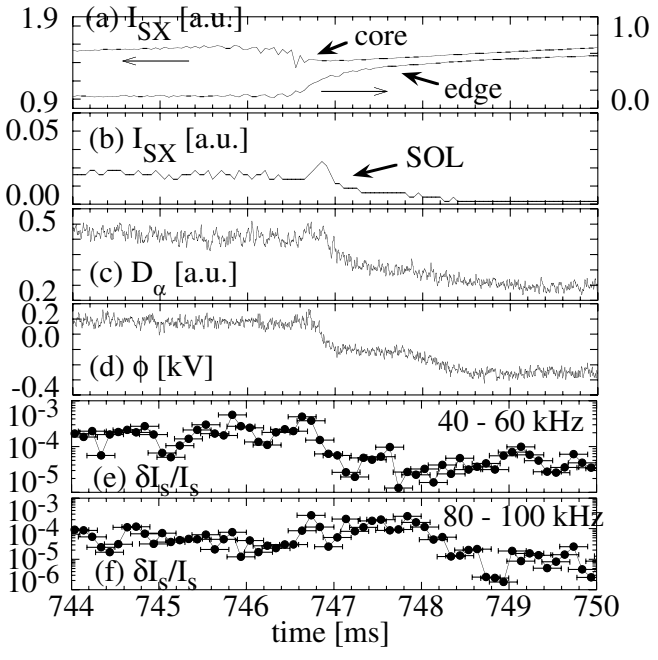

FIG. 4. The temporal evolution of potential and other plasma parameters at L-H transition. The positions of sample volumes are $ds = -2.2$ cm. (a), and (b) SX intensities from the core and the edge, and the SOL, respectively. (c) D_α intensity. (d) potential. (e) and (f) show the power of fluctuation of the secondary beam. It is integrated from 40 to 60 kHz (e) and from 80 to 100 kHz (f). The error bars indicate the time window for fast Fourier transform (320 μs).

We shall estimate the time scale of the change in ϕ quantitatively. The typical potential signals shown in Figs. 5(a) and 5(c) are the same shots as in Fig. 3 and 4, respectively. Figure 5(b) is performed in the same condition, though the position of the sample volume is more inside. Two types of changes in ϕ are observed: One is a fast change just after a sawtooth crash and the other is a relatively slow change at a few 100 μs after a sawtooth crash. The signal of ϕ is separated into three periods, labeled (i), (ii), and (iii), to estimate the time scale.

To begin with, the time scale of the drop just after the sawtooth, labeled (i), is estimated by fitting a function of $\phi(t) = \phi_L + \Delta\phi_1 \exp[-(t - t_0)/\tau_f]$, where ϕ_L, $\Delta\phi_1$,

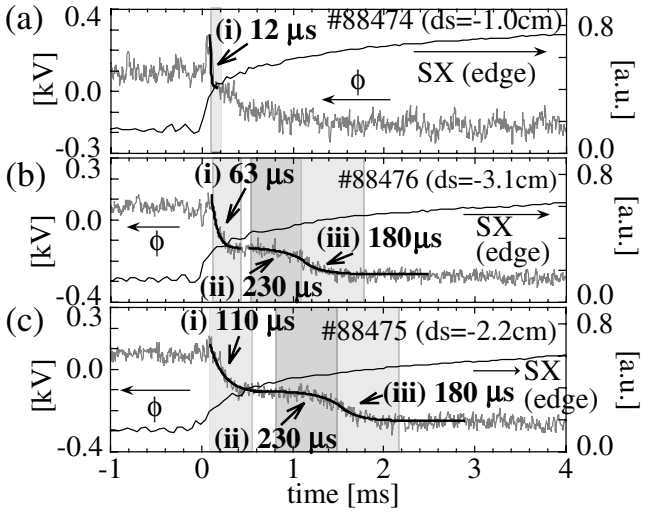

FIG. 5. Temporal behaviors of the potential and SX intensities at L-H transition. Zero [ms] means the time of the arrival of the heat pulse at the edge. The times in figures are the time scale of the potential change. The hatched periods indicate the periods used for the fitting.

t_0, and τ_f are fitting parameters and τ_f is the time scale. The estimated time scales are shown in the figures and they are in the range from 10 to about 100 μs and such time scales can be observed exactly for the first time by the HIBP.

Next, the temporal behaviors of the relatively slow change in ϕ at about 1 ms after the sawtooth crash, labeled (ii) and (iii), are a little different from that of the fast drop mentioned above. The potential seems to start to decrease exponentially and to relax in the H mode level. That is similar to the behavior of E_r evaluated from the flow velocity [10]. The time scales of the change in ϕ are estimated by fitting functions of $\phi(t) = \phi_L \mp \Delta\phi_1 \exp[\pm(t - t_0)/\tau_f]$, where the upper and lower signs are for the exponential decrease labeled (ii) and the relaxation labeled (iii). The time scales of (ii) and (iii) are about 230 and 180 μs, respectively.

The more precise measurements of other plasma parameters and the progress of theory are needed to interpret the time scales, and any conclusive statement about the mechanism of formation of E_r is not derived at present. However, one of the candidates may be as follows. In JFT-2M, an energy distribution of a charge exchange neutral flux is measured by time-of-flight (TOF) measurement and it is shown that the outward flux of collisionless deuterium ion with the energy of 300 eV and more increases at the L-H transition [24]. The bounce time of 300 eV deuterium is 50 μs with $R = 1.3$ m, $a = 0.25$ m, and the safety factor $q = 2.8$, and it seems to be comparable to the order of the time scale at the fast drop in ϕ, labeled (i). It may suggest that the rapid increase in the banana ions loss contributes the fast change in E_r, as speculated in Ref. [24]. SX intensities from the plasma edge are also shown in Fig. 4, and they reflect the magnitudes of the heat pulses caused by the sawteeth crashes. The time scale of the change in ϕ seems to depend on the magnitude of the heat pulse: a larger heat pulse induces a faster change in ϕ. Assuming that the amount of the ion loss, that is the radial current, depends on the magnitude of the heat pulse, the dependence of the time scale on the magnitude of the heat pulse is explained qualitatively.

The exponential decrease in ϕ, labeled (ii), may occur through a process mentioned below. The fluctuation starts to be stabilized by ∇E_r formed just after the arrival of the heat pulse and by the change in the profile of n_e and T_e, and the confinement is improved. Then, the profiles of n_e and T_e change further and the larger E_r is formed. They might form the positive feedback.

In summary, ϕ is measured directly at the sawtooth-triggered L-H transition by the HIBP with the high time resolution, and two types of its change are observed. One is a fast change just after a sawtooth crash and the other is a relatively slow change at a few 100 μs after a sawtooth crash. The time scale of the former is in the range from 10 to 100 μs. The time scale of the latter case is about 230 μs at the start of change and about 180 μs at the end. Although the results do not produce any conclusive statement about the mechanism of the E_r formation at present, they become a touchstone of the validity of theoretical models.

We are grateful to Professor K. Itoh and Professor S.-I. Itoh for fruitful discussions, and to Dr. H. Kimura, Dr. A. Funahashi, Dr. M. Azumi, Dr. H. Kishimoto, Professor M. Fujiwara, and Professor A. Iiyoshi for continuous encouragement. We would like to thank Professor J. D. Callen for valuable comments. T. I. is especially grateful to Professor T. Watari and Dr. A. Fujisawa for their continuous encouragement and useful discussions.

[1] S.-I. Itoh and K. Itoh, Phys. Rev. Lett. **60**, 2276 (1988).
[2] F. Wagner *et al.,* Phys. Rev. Lett. **49**, 1408 (1982).
[3] K. C. Shaing and E. C. Crume, Jr., Phys. Rev. Lett. **63**, 2369 (1989).
[4] R. J. Groebner, K. H. Burrell, and R. P. Seraydarian, Phys. Rev. Lett. **64**, 3015 (1990).
[5] K. Ida *et al.,* Phys. Rev. Lett. **65**, 1364 (1990).
[6] For review, see J. W. Connor and H. R. Wilson, Plasma Phys. Controlled Fusion **42**, R1 (2000); K. H. Burell, Phys. Plasmas **4**, 1499 (1997).
[7] H. Biglari, P. H. Diamond, and P. W. Terry, Phys. Fluids B **2**, 1 (1990).
[8] E. J. Doyle *et al.,* Phys. Fluids B **3**, 2300 (1991).
[9] K. H. Burrell *et al.,* Phys. Plasmas **1**, 1536 (1994).
[10] R. A. Moyer *et al.,* Phys. Plasmas **2**, 2397 (1995).
[11] S. Jachmich *et al.,* Plasma Phys. Controlled Fusion **40**, 635 (1998).
[12] W. Herrmann and ASDEX Upgrade Team, Phys. Rev. Lett. **75**, 4401 (1995).
[13] K. Itoh and S.-I. Itoh, Nucl. Fusion **29**, 1031 (1989).
[14] R. L. Hickok, Rev. Sci. Instrum. **38**, 142 (1967).
[15] For example, A. Fujisawa *et al.,* Phys. Rev. Lett. **82**, 2669 (1999).
[16] T. Ido *et al.,* Rev. Sci. Instrum. **70**, 955 (1999), part II.
[17] Y. Hamada *et al.,* Plasma Phys. Controlled Fusion **36**, 1743 (1994).
[18] Y. Hamada *et al.,* in *Proceedings of the 17th IAEA Fusion Energy Conference* (IAEA-F1-CN-69/PD, 1998).
[19] T. S. Green and G. A. Proca, Rev. Sci. Instrum. **41**, 1409 (1970).
[20] T. Ido *et al.,* Plasma Phys. Controlled Fusion **41**, 1013 (1999).
[21] A. Fujisawa *et al.,* Rev. Sci. Instrum. **68**, 3393 (1997).
[22] K. Ida *et al.,* Phys. Fluids B **4**, 2552 (1992).
[23] T. Ido *et al.,* Plasma Phys. Controlled Fusion **42**, A309 (2000).
[24] Y. Miura and JFT-2M Group, Nucl. Fusion **37**, 175 (1997).